Research in Astron. Astrophys. **2013** Vol. **13** No. **10**, 1155–1162
http://www.raa-journal.org *http://www.iop.org/journals/raa*

***R**esearch in*
***A**stronomy and*
***A**strophysics*

A *Chandra* study of the massive, distant galaxy cluster SDSS J0150–1005 *

Zhen-Zhen Qin[1], Hai-Guang Xu[1], Jing-Ying Wang[1] and Jun-Hua Gu[2]

[1] Department of Physics, Shanghai Jiao Tong University, Shanghai 200240, China; *qzz@sjtu.edu.cn*
[2] National Astronomical Observatories, Chinese Academy of Sciences, Beijing 100012, China

Received 2013 February 19; accepted 2013 June 1

Abstract We present a study of a fossil cluster, SDSS J0150–1005 ($z \simeq 0.364$), with high spatial resolution based on the imaging spectroscopic analysis of *Chandra* observations. The *Chandra* X-ray image shows a relaxed and symmetric morphology, which indicates that SDSS J0150–1005 is a well-developed galaxy cluster with no sign of a recent merger. According to the isothermal model, its global gas temperature is 5.73 $\pm$ 0.80 keV, and the virial mass is $6.23 \pm 1.34 \times 10^{14}\ M_{\odot}$. Compared with the polytropic temperature model, the mass calculated based on the isothermal model is overestimated by 49%$\pm$11. The central gas entropy, $S_{0.1\,r_{200}} = 143.9 \pm 18.3$ keV cm^2, is significantly lower than the average value of normal galaxy clusters with similar temperatures. Our results indicate that SDSS J0150–1005 formed during an early epoch.

Key words: galaxies: clusters: general — galaxies: evolution — galaxies: halos— intergalactic medium — X-rays: galaxies: clusters

1 INTRODUCTION

Galaxy clusters are the largest gravitationally bound systems in the universe. They originated from extreme overdensities in the primordial density field, grew through continuous accretion as well as serial mergers and finally formed mass concentrations of $10^{14}-10^{15}\ M_{\odot}$ at the present epoch. X-ray studies of galaxy clusters play an important role in establishing the current cosmological paradigm. However, it is still necessary to investigate massive, distant galaxy clusters to help determine the cosmological parameters with even higher precision.

SDSS J0150–1005 (RA = $01^{\rm h}50^{\rm m}21.3^{\rm s}$, Dec = $-10^{\circ}05'\ 31''$, J2000.0) is located at $z \simeq 0.364$. It is a massive (and thus, by inference, very X-ray luminous), distant galaxy cluster in the MAssive Cluster Survey (MACS) sample, which includes the most extreme and rarest clusters out to significant redshift (Ebeling et al. 2001). SDSS J0150–1005 was identified as a fossil system by Santos et al. (2007), in which 34 fossil systems were found from the Sloan Digital Sky Survey (Adelman-McCarthy et al. 2007). According to the definition of Jones et al. (2003), a fossil system is a gravitationally bound system with spatially extended X-ray emission, whose X-ray luminosity is higher than 1×10^{42} erg s^{-1} and $\Delta m_{12} \geq 2.0$ mag, where Δm_{12} is the gap in absolute total magnitude for the R band between the brightest and second-brightest member galaxies within half of the (projected)

* Supported by the National Natural Science Foundation of China.

virial radius. The processes of origin and evolution for fossil systems are still not well understood. In this work, we study a galaxy cluster, SDSS J0150–1005, by analyzing *Chandra* archive data to probe the X-ray properties of the fossil system in the regime of very high mass.

We describe the data reduction, imaging and spectroscopic analysis in Section 2, and discuss and summarize our results in Sections 3 and 4, respectively. Throughout this paper, we adopt the angular diameter distance of 1031.7 Mpc to the cluster using $H_0 = 71$ km s^{-1} Mpc^{-1}, $\Omega_m = 0.3$ and $\Omega_\Lambda = 0.7$. At this distance, $1'$ corresponds to 296.9 kpc. We adopt the solar abundance standards of Grevesse & Sauval (1998), where the iron abundance relative to hydrogen is 3.16×10^{-5} in number. Unless stated otherwise, the quoted errors are the 68% confidence limits.

2 DATA ANALYSIS

2.1 Observation and Data Reduction

The *Chandra* observation of SDSS J0150–1005 was carried out on 2009 September 14 (ObsID 11711) for a total exposure of 27.1 ks with CCDs 0, 1, 2 and 3 in the Advanced CCD Imaging Spectrometer (ACIS). The events were collected with an exposure time of 3.2 s and telemetered in the VeryFaint mode. The focal plane temperature was set to -120°C. We use the *Chandra* data analysis software package CIAO (version 4.5) to process the data extracted from the I chips. We keep events with *ASCA* grades 0, 2, 3, 4 and 6, and remove all the bad pixels, bad columns, columns adjacent to bad columns and node boundaries. In order to identify possible strong background flares, light curves were extracted from a box region $5.1'$ (about $1.5\,r_{500}$) away from the X-ray peak. Time intervals during the count rate exceeding the average quiescent value by 20% were excluded.

2.2 X-ray Surface Brightness

Figure 1(a) shows the raw *Chandra* ACIS-I image of SDSS J0150–1005 in the $0.7 - 7.0$ keV band, where all the point sources of the fossil cluster that could be detected at the confidence level of 3σ using the CIAO tool *celldetect* were excluded. The X-ray morphology roughly shows a relaxed and symmetric appearance.

Figure 1(b) shows the SDSS B-band image for the box region in Figure 1(a), with the *Chandra* $0.7 - 7.0$ keV X-ray intensity contours overlaid. The white plus in the center indicates the X-ray peak of SDSS J0150–1005. The X-ray peak and the position of the cD galaxy SDSS J015021.27–100530.4 are consistent with each other within $1''$. The cD galaxy shows regular morphology, and appears as a giant isolated elliptical galaxy.

The exposure-corrected surface brightness profile (SBP) is extracted from a series of annular regions centered on the X-ray emission peak, and shown in Figure 2. The energy band of the SBP is restricted to $0.7 - 7.0$ keV. Assuming spherical symmetry, we deproject the SBP to derive the three-dimensional electron number density profile $n_{\rm e}(r)$ of the intracluster medium (ICM) with the standard "*onion-skin*" method (Kriss et al. 1983). Using the single-β model, we fit $n_{\rm e}(r)$ for SDSS 0150–1005 as

$$n_{\rm e}(r) = n_0[1 + (r/r_{\rm c})^2]^{-1.5\beta} + n_{\rm bkg}, \quad (1)$$

where r is the radius, n_0 corresponds to the central electron number density, $r_{\rm c}$ is the core radius, β is the slope and $n_{\rm bkg}$ is the background. The reduced chi-square of the single-β model fit is $\chi^2/{\rm dof} = 1.88$, which is unsatisfactory. The single-β best-fit SBP (dashed line in Fig. 2) exhibits significant disagreement in the central 30 kpc due to the existence of central excess. Therefore, we apply the double-β model to describe $n_{\rm e}(r)$ as,

$$n_{\rm e}(r) = n_1[1 + (r/r_{\rm c1})^2]^{-1.5\beta_1} + n_2[1 + (r/r_{\rm c2})^2]^{-1.5\beta_2} + n_{\rm bkg}, \quad (2)$$

which gives an acceptable fit with the reduced chi-square $\chi^2/{\rm dof} = 1.04$. The double-β best-fit SBP is shown as a solid line in Figure 2. The resultant $n_1 = 0.054 \pm 0.004$ cm^{-3}, $r_{\rm c1} = 15.48 \pm 1.59$

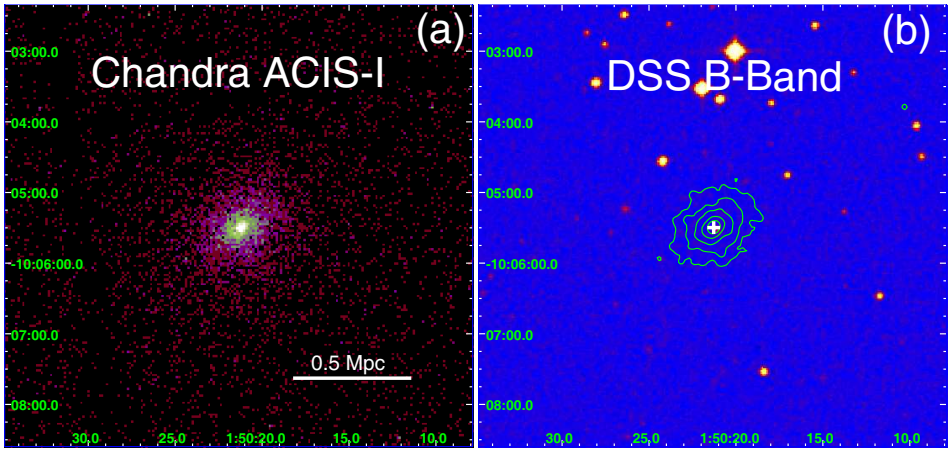

Fig. 1 (a) Raw *Chandra* image of SDSS J0150–1005 in the $0.7-7.0$ keV energy band. (b) SDSS B-band optical image for the box region in Figure 1(a), where the X-ray contours of *Chandra* $0.7-7.0$ keV image are overlaid. The white plus in the center indicates the X-ray peak of SDSS J0150–1005.

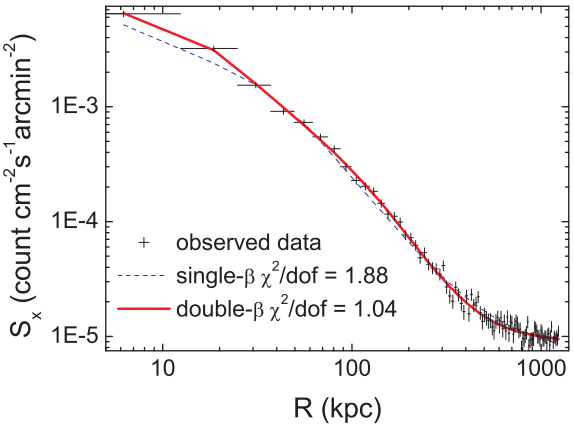

Fig. 2 Exposure-corrected surface brightness profiles extracted from a series of annular regions centered on the X-ray emission peak of SDSS J0150–1005. R is the projected distance. The blue dashed and red solid lines correspond to the best-fit single-β and double-β SBPs, respectively.

kpc and $\beta_1 = 0.65 \pm 0.02$ for one component; $n_2 = 0.005 \pm 0.001$ cm^{-3}, $r_{c2} = 107.43 \pm 14.75$ kpc and $\beta_2 = 0.64 \pm 0.02$ for the other. According to the best-fit gas distribution, the average gas density in the central 150 kpc region is $\simeq 0.005 \pm 0.001$ cm^{-3}.

2.3 Hardness Ratio Map

We define the hardness ratio as the ratio of counts within the $2.0-7.0$ keV band over that within the $0.7-2.0$ keV band. For the observations of the ICM, the hardness ratio is a temperature diagnostic: a larger hardness ratio means higher temperature. The hard-band ($2.0-7.0$ keV) and the soft-band

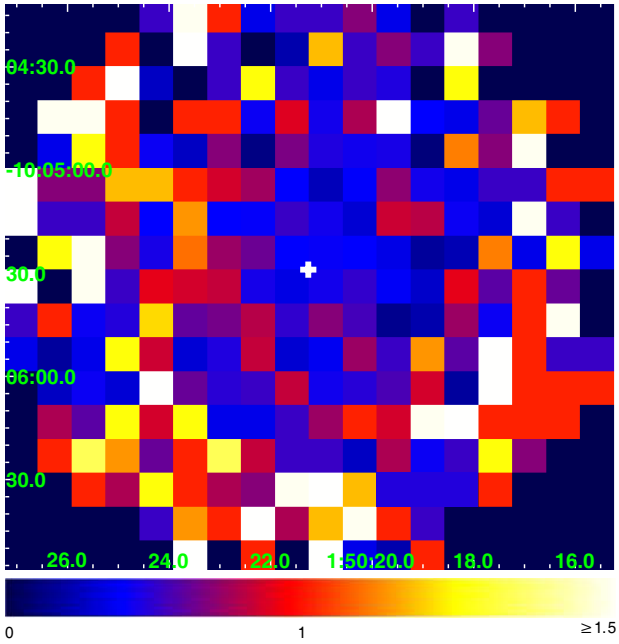

Fig. 3 Hardness ratio map (see definition in Sect. 2.3), which is binned spatially by a factor of 20. The white plus in the center indicates the X-ray peak of SDSS J0150–1005.

($0.7-2.0$ keV) counts are extracted from the event data, and then binned spatially by a factor of 20 to increase the statistical significance for every pixel.

Figure 3 exhibits the hardness ratio map, which demonstrates that SDSS J0150–1005 could be a cool core cluster, because it has a lower hard-band count in the center. Moreover, there is no obvious thermal substructure in this cluster.

2.4 Spectral Analysis

We utilize the *Chandra* blank-sky template for the ACIS CCDs as the background. The template is tailored to match the actual pointing (Pointing RA = 27.5947774587, Pointing Dec = –10.0645622317 and Pointing Roll = 81.4228143940). The background spectrum is extracted and processed identically to the source spectrum. Then, we rescale the background spectrum by normalizing its high energy end $9.0-12.0$ keV to the corresponding observed spectrum. The corresponding spectral redistribution matrix files and auxiliary response files are created by using the CIAO tools $mkacisrmf$ and $mkwarf$, respectively. All spectra are rebinned to ensure at least 20 raw counts per spectral bin to allow χ^2 statistics to be applied. Since the contribution of the hard spectral component is expected to be rather weak, and also to minimize the effects of the instrumental background at higher energies as well as the calibration uncertainties at lower energies, the fit is restricted to $0.7-7.0$ keV.

Due to the limited counts, it is insufficient to extract the deprojected temperature profile of SDSS J0150–1005. We take the spectral temperature from the annulus $0.2-0.5\,r_{500}$ as the global temperature in order to reduce the effect of a cool core (Zhang et al. 2007). r_{500} is the radius within which the average mass density is 500 times the critical density of the universe at the corresponding redshift. We will describe how to determine it in Section 3.1. We use the XSPEC 12.4.0 package to fit

the spectrum. Following the method in Gu et al. (2010), we model the gas with the WABS × APEC model. We fix the absorption to the Galactic value of 2.15 $\times 10^{20}$ cm^{-2} (Dickey & Lockman 1990). The best fit determines a temperature of 5.73 ± 0.80 keV, and an abundance of 0.30 ± 0.07 times solar with $\chi^2/\mathrm{dof} = 0.97$. As a cross check for its cool core identified with the hardness ratio map, we also extract the spectral temperature within $0.2\,r_{500}$ and fit the spectrum with the same method described above. In the cluster's center, the best-fit ($\chi^2/\mathrm{dof} = 1.02$) temperature and abundance are 4.54 ± 0.33 keV and 0.51 ± 0.14 times solar, respectively. Such a low inner temperature also indicates the cool core of SDSS J0150–1005.

3 RESULTS

3.1 Total Gravitational Mass Profile

In a spherically symmetric system in hydrostatic equilibrium, $M_{\mathrm{tot}}(< r)$, the total mass within a given radius, r, is given by

$$M_{\mathrm{tot}}(< r) = -\frac{k_{\mathrm{B}}T(r)r}{G\mu m_{\mathrm{p}}}\left[\frac{d\,\mathrm{ln}n_{\mathrm{e}}(r)}{d\,\mathrm{ln}r} + \frac{d\,\mathrm{ln}T(r)}{d\,\mathrm{ln}r}\right], \quad (3)$$

where G is the universal gravitational constant, k_{B} is the Boltzmann constant, $\mu = 0.62$ is the mean molecular weight per hydrogen atom, m_{p} is the proton mass, $n_{\mathrm{e}}(r)$ is the electron number profile, and $T(r)$ is the temperature profile. In the $M_{\mathrm{tot}}(< r)$ calculation, n_{e} is obtained from the best fit of the X-ray surface brightness profile described in Section 2.2. As described in Section 2.4, we cannot acquire the deprojected temperature profile of SDSS J0150–1005. Therefore, we assume that this cluster is an isothermal system. In such a case, there is an iterative process involved in the mass calculation: an initial r_{500} is provided to obtain the global temperature; the global temperature is then used in Equation (3) to produce r_{500} for the next iteration; such iteration continues until r_{500} and the global temperature converges. Based on the resultant global temperature, the virial radius r_{200} and virial mass M_{200} are obtained. With Equation (3) and 1000 Monte Carlo simulations, virial radius is r_{200} = 1.54 ± 0.11 Mpc and the virial mass is $6.23 \pm 1.34 \times 10^{14}\ M_{\odot}$. The total gravitational mass profile is shown in Figure 4.

We assume there is an isothermal distribution that may overestimate the mass of the galaxy's cluster. In order to constrain this uncertainty, we also adopt the polytropic model (Sarazin 1988), where the temperature gradient in the intracluster gas is assumed. In this model, if the hot gas is strictly adiabatic, its pressure and density have a simple relation of $P \propto \rho_{\mathrm{gas}}^{\gamma}$, where polytropic index γ is the usual ratio of specific heat. Because of the low density ($n_{\mathrm{e}} < 10^{-2}$ cm^{-2}), the ICM can be treated as an ideal gas with $P = n_{\mathrm{gas}}k_BT$. The temperature profile is described by

$$T(r) = T_{0,\gamma}\left(\frac{\rho_{\mathrm{gas}}(r)}{\rho_0}\right)^{\gamma-1} = T_{0,\gamma}\left(\frac{n_{\mathrm{e}}(r)}{n_0}\right)^{\gamma-1}. \quad (4)$$

As a rough estimation, we adopt the polytropic index $\gamma = 1.19 \pm 0.03$ according to Tawa (2008), in which they used observations from the Suzaku satellite and extended the temperature profiles up to the virial radius. The resultant virial mass is $4.20 \pm 1.01 \times 10^{14}\ M_{\odot}$, and the calculated total gravitational mass profile is also shown in Figure 4. We find that the virial mass derived from the isothermal model is overestimated by $49\% \pm 11$ compared with the polytropic temperature model.

3.2 Gas luminosity

The luminosity, L_{X}, of SDSS J0150–1005 within r_{200} is given by $L_{\mathrm{X}} = \iiint \Lambda n_{\mathrm{e}} n_{\mathrm{H}} dV$, where Λ is the cooling function and n_{H} is the proton number density. We calculate the integral of the electron number density profile to get the bolometric $L_{\mathrm{X}} = 3.87 \pm 1.47 \times 10^{44}$ erg s^{-1}. The error of L_{X} is obtained from the Poisson error in the X-ray count rate.

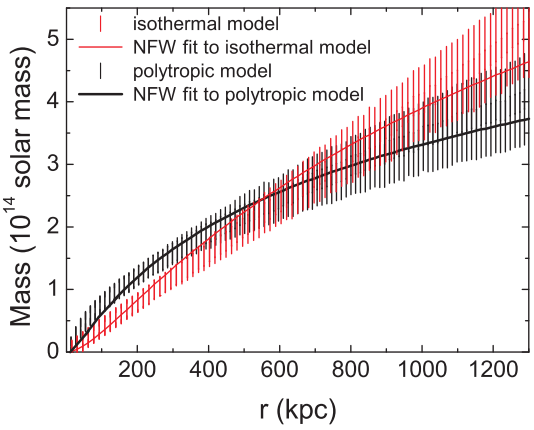

Fig. 4 Total gravitational mass profiles of SDSS J0150–1005 based on isothermal (*red*) and polytropic (*black*) temperature models (*color online*). The solid lines show the best fits to the NFW model, which give mass concentration parameters $c_{200} = 8.55 \pm 0.38$ and 22.46 ± 1.33 for the isothermal and polytropic temperature models, respectively.

4 DISCUSSION

According to results presented in Section 3, we would like to discuss the epoch of formation for SDSS J0150–1005 through X-ray morphology, the mass concentration parameter and the central entropy as follows.

The X-ray morphology of SDSS J0150–1005 shows a relaxed and symmetric appearance: the cD galaxy is consistent with the X-ray peak within $1''$; there exists a cool core in the center of the galaxy cluster, as shown in the hardness ratio map; and also no clumps or substructure are seen in the ICM. The simulation of Poole et al. (2006) claims that the system needs $\sim 2 \times 10^9$ yr to relax and virialize, and that the smoothness of isophotes in its X-ray surface brightness is the only reliable indicator of the virialization. Therefore, this galaxy cluster exhibits no violent turbulence caused by recent major mergers.

We apply the NFW profile (Navarro et al. 1995)

$$\rho(r) = \frac{\rho_0 \delta_{\rm c}}{(r/r_{\rm s})(1 + r/r_{\rm s})^2}, \tag{5}$$

to describe the total gravitational mass density, where ρ is the mass density, $r_{\rm s}$ is the scale radius, ρ_0 is the critical density of the universe, and $\delta_{\rm c}$ is the characteristic density. With the NFW model, we can obtain the following integrated profile of a spherical mass distribution,

$$M_{\rm tot}(< r) = 4\pi\delta_{\rm c}\rho_0 r_{\rm s}^3 \left[\ln\left(1 + \frac{r}{r_{\rm s}}\right) - \frac{r}{r + r_s}\right]. \tag{6}$$

We fit the NFW mass profile, Equation (6), to the total gravitational mass profile, derived from X-rays in the isothermal model, obtained in Section 3.1, and the result is shown in Figure 4. The best-fit gives $r_{\rm s} = 181.24 \pm 11.20$ kpc. The mass concentration parameter is defined as $c_{200} = r_{200}/r_{\rm s} = 8.55 \pm 0.38$. Due to the systematic overestimation of the mass distribution by the isothermal model, we also apply the NFW mass profile to the total gravitational mass profile derived by the polytropic temperature model in Section 3.1; the resultant $r_{\rm s} = 60.48 \pm 5.86$ kpc and $c_{200} = 22.46 \pm 1.33$. Both concentration parameters are higher than the simulated and observed values in galaxy clusters with

similar mass (Dolag et al. 2004; Pratt & Arnaud 2005). Simulation shows that dark matter halos, which have not undergone a major merger since $z = 2$, are more concentrated than those that have experienced one since then (Wechsler et al. 2002). Such a high mass concentration may indicate an early epoch of formation.

The gas entropy is defined as

$$S = T/n_{\rm e}^{2/3}. \quad (7)$$

We focus on the gas entropy at $0.1\,r_{200}$, $S_{0.1\,r_{200}}$. Because $0.1\,r_{200}$ is very close to the center, we can avoid entropy generated from the shock, and thus enhance the sensitivity to any additional entropy. This yields $S_{0.1\,r_{200}} = 143.9 \pm 18.3$ keV cm^2, which is significantly lower than the average value obtained by Pratt et al. (2006) for the relaxed galaxy clusters with similar temperatures. Voit et al. (2003) suggested that most feedback within the ICM occurs before it falls into the clusters, rather than after virialization. In the pre-collapse gas, the high contrast in density leads to higher post-shock entropy, once the gas crosses the accretion shock during the formation of the galaxy cluster. According to the above statements, we conclude that the lower gas entropy in the center also indicates an early epoch of formation for this galaxy cluster.

As discussed above, SDSS J0150–1005 shows no recent major mergers or early formation according to its relaxed X-ray morphology, high mass concentration and low central entropy. From the simulation by D'Onghia et al. (2005), a fossil system should have already assembled half of its final mass at $z \sim 1$, and subsequently it typically only grows by minor mergers. The high mass concentration was also previously reported in other fossil systems (Khosroshahi et al. 2004, 2006; Sun et al. 2004). Moreover, the gas entropy in fossil systems is reported to lie along the lower envelope of the entropy-temperature distribution (Khosroshahi et al. 2007). Therefore, we conclude that the X-ray properties of SDSS J0150–1005 may be ascribed to its fossil character.

5 SUMMARY

With the *Chandra* observation of a massive, distant galaxy cluster, SDSS J0150–1005, we study properties of this fossil cluster related to hot gas, including its temperature, luminosity and gas entropy. The isothermal and polytropic temperature models are adopted to estimate the total gravitational mass. Its relaxed X-ray morphology, high mass concentration parameter and low entropy near its center indicate that this cluster formed early and has not experienced a recent major merger. We conclude that these X-ray properties may be ascribed to its fossil character.

Acknowledgements We thank the anonymous referee for useful suggestions on the manuscript. This work was supported by the National Basic Research Program of China (973 Program; Grant Nos. 2009CB824900 and 2009CB824904), the National Natural Science Foundation of China (Grant Nos. 10878001, 10973010 and 11125313), and the Shanghai Science and Technology Commission (Program of Shanghai Subject Chief Scientist; Grant Nos. 12XD1406200 and 11DZ2260700).

References

Adelman-McCarthy, J. K., Agüeros, M. A., Allam, S. S., et al. 2007, ApJS, 172, 634
Dickey, J. M., & Lockman, F. J. 1990, ARA&A, 28, 215
Dolag, K., Bartelmann, M., Perrotta, F., et al. 2004, A&A, 416, 853
D'Onghia, E., Sommer-Larsen, J., Romeo, A. D., et al. 2005, ApJ, 630, L109
Ebeling, H., Edge, A. C., & Henry, J. P. 2001, ApJ, 553, 668
Grevesse, N., & Sauval, A. J. 1998, Space Sci. Rev., 85, 161
Gu, L.-Y., Wang, Y., Gu, J.-H., et al. 2010, RAA (Research in Astronomy and Astrophysics), 10, 1005
Jones, L. R., Ponman, T. J., Horton, A., et al. 2003, MNRAS, 343, 627
Khosroshahi, H. G., Jones, L. R., & Ponman, T. J. 2004, MNRAS, 349, 1240

Khosroshahi, H. G., Maughan, B. J., Ponman, T. J., & Jones, L. R. 2006, MNRAS, 369, 1211
Khosroshahi, H. G., Ponman, T. J., & Jones, L. R. 2007, MNRAS, 377, 595
Kriss, G. A., Cioffi, D. F., & Canizares, C. R. 1983, ApJ, 272, 439
Navarro, J. F., Frenk, C. S., & White, S. D. M. 1995, MNRAS, 275, 720
Poole, G. B., Fardal, M. A., Babul, A., et al. 2006, MNRAS, 373, 881
Pratt, G. W., & Arnaud, M. 2005, A&A, 429, 791
Pratt, G. W., Arnaud, M., & Pointecouteau, E. 2006, A&A, 446, 429
Santos, W. A., Mendes de Oliveira, C., & Sodré, L., Jr. 2007, AJ, 134, 1551
Sarazin, C. L. 1988, X-ray Emission from Clusters of Galaxies, Cambridge Astrophysics Series (Cambridge: Cambridge Univ. Press)
Sun, M., Forman, W., Vikhlinin, A., et al. 2004, ApJ, 612, 805
Tawa, N. 2008, PhD Thesis (Osaka University), *http://www.astro.isas.jaxa.jp/suzaku/bibliography/phd/*
Voit, G. M., Balogh, M. L., Bower, R. G., Lacey, C. G., & Bryan, G. L. 2003, ApJ, 593, 272
Wechsler, R. H., Bullock, J. S., Primack, J. R., Kravtsov, A. V., & Dekel, A. 2002, ApJ, 568, 52
Zhang, Y.-Y., Finoguenov, A., Böhringer, H., et al. 2007, A&A, 467, 437